ACOUSTIC SCATTERING FROM ELLIPSES BY THE MODAL ELEMENT METHOD

Kevin L. Kreider
The University of Akron
Department of Mathematical Sciences
Akron, Ohio 44325-4002

and

Kenneth J. Baumeister
National Aeronautics and Space Administration
Lewis Research Center
Cleveland, Ohio 44135

ABSTRACT

The modal element method is used to study acoustic scattering from ellipses, which may be acoustically soft (absorbing) or hard (reflecting). Because exact solutions are available, the results provide a benchmark for algorithm performance for scattering from airfoils and similar shapes. Numerical results for scattering from rigid ellipses are presented for a wide variety of eccentricities at moderate frequencies. These results indicate that the method is practical.

INTRODUCTION

Acoustic and electromagnetic scattering from airfoils is of interest to the aerospace industry in, for example, studies of noise abatement and identification by radar signature. The study of scattering from cylinders and bodies embedded in circular cylinders using the modal element method was recently presented by Baumeister and Kreider (1993a). The modal element method is a computationally efficient formulation in which both analytical and finite element solutions are combined. This study is concerned with scattering from ellipses using the modal element method. The elliptic geometry can be computationally efficient in many aeronautic applications. For example, thin airfoil shapes can be more naturally embedded in an ellipse than in a circle.

The modal element method has been employed in electromagnetic and acoustic scattering and duct transmission problems (Baumeister and Baumeister (1994), Baumeister and Kreider (1993a), Baumeister and Kreider (1993b), Lee & Cendes (1987), Astley and Eversman (1981), and Chang & Mei (1976), for example). In this method, the acoustic pressure or electromagnetic field in and on the scattering body is represented by finite elements (the finite element solution), while the field is represented by an eigenfunction expansion away from the body (the modal solution). The two solution forms are coupled through an interface condition.

The purpose of this paper is to present the results of the study of acoustic scattering from ellipses using an elliptic interface rather than a circular one. The modal element method using an elliptic interface can be used effectively to study scattering from airfoil shapes for two reasons. First, if the far field results match the exact solution for hard ellipses of high eccentricity, it can be inferred that the method can be applied to scattering from a similar shape, such as an airfoil. Second, airfoils can be more efficiently embedded in an ellipse than in a circle, which decreases the size of the finite element domain, saving computation time and lessening computer memory requirements. For example, a reduction of grid size by 10 yields a savings in the global matrix size of 100.

There have been many recent studies of scattering from ellipses and more complicated shapes using other analytical methods; among them are Kim (1991), Jin and Liepa (1988), and Rojas (1988). The present work adds to these studies by allowing more flexibility in setting absorbing material around the surface of the ellipse.

The numerical results presented here are for scattering from hard ellipses. The modal element method could also be used for scattering from soft ellipses, with the modifications mentioned under Results.

SOLUTION METHOD

The goal here is to compute numerically the acoustic scattering of a plane wave, travelling in the +x direction, that strikes an ellipse. The spatial domain is divided into two subdomains, the finite element domain, which contains the body, and the homogeneous domain, which surrounds the body and extends to infinity (fig. 1). Linear triangular elements are used in the finite element domain to calculate the pressure at the nodes (the finite element solution). In the homogeneous domain, an eigenfunction expansion with unknown modal coefficients represents the acoustic pressure (the modal solution). The two solution forms are coupled by imposing continuity on the pressure and velocity at the elliptical interface between the two subdomains. This coupling results in a single matrix equation in which the eigenfunction coefficients and the pressures at the finite element nodes are calculated simultaneously, yielding a global representation of the acoustic field.

GEOMETRICAL MODEL

For the numerical studies done here, the scattering ellipse is taken to be rigid; in this case, it can be represented by a thin ring of finite elements as shown in figure 2. The elliptic co-ordinate system used is shown in figure 3. The variables are standard:

$$
\begin{aligned}
x &= \frac{d}{2}\cosh u \ \cos v \\
y &= \frac{d}{2}\cosh u \ \sin v \\
z &= z \\
\xi &= \cosh u, \quad \eta = \cos v
\end{aligned}
\tag{1}
$$

In (u,v) co-ordinates, u is the radial and v is the angular component; in (ξ,η) co-ordinates, ξ is the radial and η is the angular component. The semi-major and semi-minor axes are denoted a and b, respectively, and $d = 2\,(a^2-b^2)^{1/2}$ is the interfocal distance. The major axis is oriented along the x axis. The eccentricity of the ellipse is defined as

$$
e = \frac{d}{2a} = \frac{1}{\xi}. \tag{2}
$$

GOVERNING EQUATION

Acoustic propagation in two dimensional space can be modeled by the continuity, momentum, and state linearized gas dynamic equations in the absence of flow. For harmonic pressure propagation in an inhomogeneous material, the following dimensionless wave equation applies:

$$\frac{\partial}{\partial x}\left(\frac{1}{\varepsilon}\frac{\partial p}{\partial x}\right)+\frac{\partial}{\partial y}\left(\frac{1}{\varepsilon}\frac{\partial p}{\partial y}\right)+\omega^2\mu p=0. \tag{3}$$

The harmonic time dependence $e^{-i\omega t}$ has been factored out. In analogy with electromagnetic scattering, ε is the acoustic "permittivity", μ is the acoustic "permeability" and ω is the dimensionless frequency. Details of these acoustic properties can be found in Baumeister and Dahl (1987). The wave number is

$$k=\sqrt{\omega^2\mu\varepsilon}. \tag{4}$$

At the interface between the finite element region and the analytic region, continuity is imposed on the pressure and velocity. The radiation boundary condition at infinity is automatically satisfied by the eigenfunction expansion introduced in the next section.

ANALYTIC SOLUTION

In the homogeneous domain, an exact eigenfunction expansion can be derived from equation (3) by separation of variables. In elliptic co-ordinates, the eigenfunctions are the Mathieu functions. A plane wave with incident angle ϕ_0 that strikes the rigid ellipse generates a pressure field written as (Bowman, et al., (1969), pg. 146, equation (3.76))

$$p_a=p^i+p^s=e^{ik(x\cos\phi_o+y\sin\phi_o)}-\sqrt{8}\pi\sum_{m=0}^{\infty}i^m\left(\frac{1}{N_m^{(e)}}\frac{Re_m^{(1)'}(c,\xi_1)}{Re_m^{(3)'}(c,\xi_1)}Re_m^{(3)}(c,\xi)\,Se_m(c,\cos\phi_o)\,Se_m(c,\eta)\right.$$
$$\left.+\frac{1}{N_m^{(o)}}\frac{Ro_m^{(1)'}(c,\xi_1)}{Ro_m^{(3)'}(c,\xi_1)}Ro_m^{(3)}(c,\xi)\,So_m(c,\cos\phi_o)\,So_m(c,\eta)\right) \tag{5}$$

p^i is the incident plane wave, p^s is the scattered field, c = kd/2 and ϕ_0 is measured counterclockwise from the +x axis. ξ_1 represents the surface of the ellipse, while the observation point (ξ,η) is exterior to the ellipse. The even and odd radial Mathieu functions of the first $\left(Re_m^{(1)}, Ro_m^{(1)}\right)$ and third $\left(Re_m^{(3)}, Ro_m^{(3)}\right)$ kinds are analogous, respectively, to the Bessel functions J_m and the Hankel function of the first kind $H_m^{(1)}$ for polar co-ordinates. The even and odd angular Mathieu functions (Se_m, So_m) are analogous to the cosine and sine functions, respectively, in polar co-ordinates. The normalization factors, $N_m^{(e)}$ and $N_m^{(o)}$ are defined by Stratton (1941, equations (18) and (19) pg. 376).

If the incident angle ϕ_0 is set to 0, equation (5) simplifies to

$$p_a=p^i+p^s=e^{ikx}-\sqrt{8}\pi\sum_{m=0}^{\infty}i^m\left(\frac{1}{N_m^{(e)}}\frac{Re_m^{(1)'}(c,\xi_1)}{Re_m^{(3)'}(c,\xi_1)}Re_m^{(3)}(c,\xi)\,Se_m(c,\eta)\right) \tag{6}$$

This exact solution (eq. (5) or (6)) is used to validate the modal element solution. In general, the scattered field is represented by

$$p^s = \sum_{m=0}^{M_{coef}-1} A_m^+ Re_m^{(3)}(c,\xi) Se_m(c,\eta) + B_m^+ Ro_m^{(3)}(c,\xi) So_m(c,\eta) \tag{7}$$

where the unknown coefficients A^+_m and B^+_m are to be determined by solving the global matrix equation. If the incident angle $\phi_0 = 0$, then the odd terms vanish ($B^+_m = 0$). If the incident angle is nonzero, or if the scatterer is not symmetric about the x axis, then the odd terms must be included.

Formulas to estimate the number of modes M_{coef} needed for convergence for scattering from circles can be found in Baumeister and Kreider (1993a). As the eccentricity of the ellipse increases, this number increases to a limit of roughly twice the value for circles.

The numerical calculation of Mathieu functions is challenging. There are several sets of accepted notation and several types of normalization of the functions. The functions are represented as a series, each term of which depends on an eigenvalue that must be calculated by solving an equation involving a continued fraction. Details of the theory of Mathieu functions may be found in Magnus, et al., (1966). Details of the numerical calculation of Mathieu functions may be found in Blanch (1964), Canosa (1971), Clemm (1969), Hirsch (1972) and Toyama and Shogen (1984). Clemm's algorithm, as improved by Hirsch, was adapted for use in this study.

INTERFACE CONDITIONS

At the interface S between the finite element domain and the homogeneous domain, both pressure and velocity are continuous (Temkin, 1981, pg. 80). The continuity of pressure

$$p|_{S^+} - p|_{S^-} = 0 \tag{8}$$

is expressed numerically by an integral weighting procedure, so the continuity of pressure at the interface is represented by the set of equations

$$\oint_{S,\ \theta=0}^{\theta=2\pi} W_{m^*}\left[p_a - p\right] ds = 0 \qquad W_{m^*} = Se_{m^*}(c,\eta), \qquad m^* = 0,1,2,\ldots,M_{coef} - 1 \tag{9}$$

There must be one weight equation for each unknown in eqn (7); if odd terms are included then additional weights $So_m(c,\eta)$ are introduced.

The choice of weight functions is crucial, since, as discussed under Results, the solution is quite sensitive to the weights used. The natural choice is to use $W_m = Se_m$, since the angular Mathieu functions are orthogonal over the surface of the ellipse (Abramowitz and Stegun (1972), section 20.5). However, this choice does not give perfect results, so that possibly a better choice of weights could be found, although after some experimentation, it seems unlikely.

The integration element ds in equation (9) is given by

$$ds^2 = r^2 d\theta^2 + dr^2 = \frac{b^2}{1 - e^2\cos^2\theta}\left(1 + \frac{e^4\cos^2\theta\sin^2\theta}{\left(1 - e^2\cos^2\theta\right)^2}\right) d\theta^2 \tag{10}$$

where the radius at any point on the ellipse is

$$r^2 = \frac{b^2}{1 - e^2 \cos^2 \theta}. \tag{11}$$

The discretization of these equations, as well as the imposition of the continuity of the pressure gradient across S, is done as in Baumeister and Kreider (1993a).

FINITE ELEMENT SOLUTION

The finite element domain is divided into triangular elements with unknown acoustic pressure at the nodes. It is assumed that all material properties are constant in each element. The setup of the global matrix follows the derivation in Baumeister and Kreider (1993a).

The weak finite element formulation of equation (3) contains a surface integral with the normal derivative of p, which is equated to the normal derivative of p_a. The normal derivative of the scattered field

$$p^s = \sum_{m=0}^{M_{coef}-1} A_m^+ Re_m^{(3)}(u) \quad Se_m(v) \tag{12}$$

requires some explanation. Notice that the notation for the arguments of the Mathieu functions has been streamlined, and uses (u,v) co-ordinates instead of (ξ,η), to be consistent with the computer code. It is convenient to write the normal derivative in terms of rectangular co-ordinates

$$\frac{\partial p^s}{\partial n} = \frac{\partial p^s}{\partial x}\cos\beta + \frac{\partial p^s}{\partial y}\sin\beta \tag{13}$$

where β is the angle between the normal to the surface and the horizontal. The code can provide the values of dp^s/du and dp^s/dv, so by writing

$$\begin{aligned} \frac{\partial p^s}{\partial x} &= \frac{\partial p^s}{\partial u}\frac{\partial u}{\partial x} + \frac{\partial p^s}{\partial v}\frac{\partial v}{\partial x} \\ \frac{\partial p^s}{\partial y} &= \frac{\partial p^s}{\partial u}\frac{\partial u}{\partial y} + \frac{\partial p^s}{\partial v}\frac{\partial v}{\partial y} \end{aligned} \tag{14}$$

it remains only to determine du/dx, du/dy, dv/dx and dv/dy. This is done by differentiating the transformation equations (1) each with respect to x and y to obtain

$$\begin{pmatrix} 1 \\ 0 \\ 0 \\ 1 \end{pmatrix} = \begin{pmatrix} A & 0 & -B & 0 \\ 0 & A & 0 & -B \\ B & 0 & A & 0 \\ 0 & B & 0 & A \end{pmatrix} \begin{pmatrix} \dfrac{\partial u}{\partial x} \\ \dfrac{\partial u}{\partial y} \\ \dfrac{\partial v}{\partial x} \\ \dfrac{\partial v}{\partial y} \end{pmatrix} \tag{15}$$

where $A = d \sinh u \cos v$ and $B = d \cosh u \sin v$. This 4 by 4 block matrix is easily inverted to give the desired quantities. Substituting them into equation (14) and then equation (13) gives the final form of the normal derivative

$$\frac{\partial p^s}{\partial n} = \left(\frac{\cos\beta \sinh u \ \cos v + \sin\beta \ \cosh u \ \sin v}{d\left(\sinh^2 u \ \cos^2 v + \cosh^2 u \ \sin^2 v\right)} \right) \sum A_m^+ \left(Re_m^{(3)}(u) \right)' Se_m(v)$$

$$+ \left(\frac{-\cos\beta \cosh u \ \sin v + \sin\beta \ \sinh u \ \cos v}{d\left(\sinh^2 u \ \cos^2 v + \cosh^2 u \ \sin^2 v\right)} \right) \sum A_m^+ Re_m^{(3)}(u) \, Se_m'(v) \tag{16}$$

where the primes signify derivatives with respect to the arguments.

RESULTS

Three examples were chosen to illustrate the behavior of the modal element method when applied to scattering from ellipses. In Example 1, the scattered pressure in the near field is shown for a range of eccentricities. Example 2 shows the near and far scattered fields for a higher frequency. In Example 3, the finite element solution is compared to the modal solution at the surface of the ellipse.

In each of the examples, the ellipse is defined with semi-major axis $a = 1$ (oriented along the x axis), and the semi-minor axis b varies between 0 and 1 to change the eccentricity. Near and far field polar plots (Examples 1 and 2) are taken on circles of the indicated radius to conform to usual far field results, while the surface plots of Example 3 are taken on the surface of the ellipse. The incident plane wave travels in the +x direction with a fixed frequency.

In the examples, the ellipse is taken to be hard, which is simulated numerically through an impedance mismatch induced by setting $\varepsilon = 1 - 10^{19}i$ and $\mu = 1$ for each internal finite element. This feature allows greater flexibility in the numerical implementation of the method, because penetrable or coated rigid bodies may be studied with only slight modifications to the computer code, mainly in grid generation. For penetrable bodies, the internal grid is more extensive, while for coated bodies, several rings in the coating region may be needed.

For examples with wave number k = 1, there are 264 grid points and 11 modal terms used, while for those with wave number k = 5, there are 384 grid points and 16 modal terms used. For all examples, the incident angle ϕ_0 is set to 0 and the thickness of the ring (fig. 2) is set to 0.001.

Example 1—Varying The Eccentricity Of The Ellipse.—The incident plane wave has wave number $k = 1$. Figures 4(a) to (d) show the modal solution for the scattered pressure field in the near field for a set of ellipses of increasing eccentricity. The exact solutions are represented by solid lines. As seen in figure 4, the errors increase slightly as b gets smaller (thinner ellipse). However, even for the most elongated scatterer, the method successfully calculates the field. For this reason, it is believed that the calculation of the far field pressure field from a realistic airfoil shape would be trustworthy.

Example 2—Near And Far Fields At Higher Frequency.—The incident plane wave has wave number $k = 5$ with semi-major axis $a = 1$ and semi-minor axis $b = 0.5$. Figures 5(a) to (d)show polar plots of the modal solution around circles of increasing radius. The exact solutions are represented by solid lines. It is clear that the solution improves farther from the scatterer, which is a consequence of the fact that the convergence properties of equation (7) improve as ξ (or u) increases. If only the far field is desired, a relatively coarse grid and fewer modal terms can be used. In the near field, more terms are required to obtain the same level of accuracy (Baumeister and Kreider 1993a, fig 4). Of course, as the frequency increases, a finer finite element grid and more modal terms must be used, leading to a larger global matrix and longer computation times.

Example 3—Comparison Of Finite Element And Modal Solutions.—The incident plane wave has wave number $k = 1$ with semi-major axis $a = 1$ and semi-minor axis $b = 0.8$. Figures 6(a) and (b) show the scattered pressure field at the surface of the ellipse based on the finite element (fig. 6(a)) and the modal (fig. 6(b)), solutions. The exact solutions are represented by solid lines. Previously, as has been shown in figures 4 and 5, the modal element solution has been shown to be very accurate in the far field. Now, as seen in figure 6(b), the modal element solution is quite good in the near field on the surface of the ellipse.

However, the finite element solution is clearly inadequate. For more elongated ellipses, the finite element solution is much worse, while the modal solution shows only a slight degradation in quality.

The reason for this disparity is that the finite element solution is sensitive to the choice of weights used in the interface condition (9). The natural choice is the set of angular Mathieu functions Se_m, but when this set (or variations such as cosine functions or phase shifted Mathieu or cosine functions) is used, the interface condition is satisfied globally but not locally. This means that although

$$\sum_{\text{boundary nodes}} p_i - p_a(x_i) = 0 \tag{17}$$

it is not true that

$$\sum_{\text{boundary nodes}} |p_i - p_a(x_i)| = 0. \tag{18}$$

The finite element solution oscillates around the exact solution in such a way that the global condition is satisfied. Since the modal coefficients depend on the global condition, the modal solution is good even when the finite element solution is not.

Attempts were made to strengthen the interface condition. First, different weights, including cosine functions and various phase shifted cosine functions, were used without success. Next, the condition itself was modified, by adding a tangential derivative:

$$\int_s W_m\left((p - p_a) + \frac{\partial}{\partial s}(p - p_a)\right) ds \tag{19}$$

But, by integrating the new term by parts, it is easy to see that the net effect is slight—for cosine weights, for example, the new weight is simply a phase shifted cosine. In all the trials, there was no improvement gained by changing the weights. In addition, changing the number of boundary nodes used in the quadrature scheme (in general, it is not necessary to use them all) had virtually no effect on the results.

For scattering from hard bodies, this error in the finite element solution is irrelevant, since the modal solution accurately portrays the scattered field. For scattering from soft bodies, however, the internal field may be important, and the algorithm must be improved. There are two possible approaches to resolve the difficulty.

First, the following iterative scheme could be implemented. After solving for the modal solution on the boundary, the internal field could be solved by using that solution as a Dirichlet boundary condition, and solving only for the finite element unknowns inside the body.

Second, the condition could be made more stringent by giving up linearity. Possible forms are

$$\sum_{\text{boundary nodes}} (p_i - p_a(x_i))^2 = 0, \quad \sum_{\text{boundary nodes}} |p_i - p_a(x_i)| = 0. \tag{20}$$

The resulting equations could be solved by a standard nonlinear system solver, but at greater computational expense.

The numerical results can be summarized as follows:

1. As the eccentricity of the ellipse and/or the incidient frequency increases, the problem requires a finer finite element grid and more modal terms. For the problems considered, the total number of unknowns ranged from 275 to 400, and the results shown are quite good.

2. Far field results are better than near field results in all cases, because the modal series (eq. (7)) requires fewer terms to converge in the far field than in the near field.

3. The finite element solution on the scattering body is often much poorer than the modal solution. This is due to sensitivity in the form of the interface condition. For hard scatterers, this is not a problem, while for soft scatterers, the algorithm can be modified to obtain the internal field.

CONCLUSION

A study of acoustic scattering by ellipses using the modal element method has been presented. The method yields acceptable numerical results for scattering from hard ellipses of any eccentricity for a range of moderate frequencies. For soft ellipses, the method must be modified to obtain the internal field. The numerical cases presented are used as validation for the method, and indicate that when applied to scattering from realistic airfoil shapes, the modal element method should yield accurate results. In addition, the airfoil can be embedded in an ellipse rather than a circle, decreasing the size of the finite element grid, and hence reducing the computing requirements for the problem.

REFERENCES

Abramowitz, M. and Stegun, I., 1972, "Handbook of Mathematical Functions," Dover Press, New York.

Astley, R.J. , and Eversman, W., 1981, "Acoustic Transmission in Non-Uniform Ducts with Mean Flow, Part II: The Finite Element Method," Journal of Sound and Vibration, Vol. 74, pp. 103–121.

Baumeister, K.J. and Baumeister, J.F., "Modal Element Method for Potential Flow in Non-Uniform Duct: Combining Closed Form Analysis With CFD," AIAA Paper 94–0813.

Baumeister, K.J. and Dahl, M.D., 1987, "A finite element model for wave propagation in an inhomogeneous material including experimental validation," AIAA Paper 87–2741 (also NASA TM–100149).

Baumeister, K.J. and Kreider, K.L., 1993a, "Modal Element Method for Scattering and Absorbing of Sound by Two-Dimensional Bodies," Journal of Vibration and Acoustics, Vol. 115, pp. 314–323.

Baumeister, K.J. and Kreider, K.L., 1993b, "Modal Ring Method for the Scattering of Sound," NASA TM–106342.

Bowman, J.J., Senior, T.B.A. and Uslenghi, P.L.E., 1969, "Electromagnetic and Acoustic Scattering by Simple Shapes," North-Holland Publishing Company, Amsterdam.

Blanch, G., 1964, "Numerical Evaluation of Continued Fractions," SIAM Review, pp. 383–421.

Canosa, J., 1971, "Numerical Solution of Mathieu's Equation," Journal of Computational Physics, Vol. 7, pp. 255–272.

Chang, S.K. and Mei, K.K., 1976, "Application of the Unimoment Method to Electromagnetic Scattering of Dielectric Cylinders," IEEE Transactions on Antennas and Propagation, pp. 35–42.

Clemm, D., 1969, "Characteristic Values and Associated Solutions of Mathieu's Differential Equation," Communications of the ACM, Vol. 12, pp. 399–407.

Hirsch, C., 1972, "Computation of Individual Characteristic Values and Associated Solutions of Mathieu's Equation," Vrije Universiteit Te Brussel, Report VUB–STR–1.

Jin, J.M. and Liepa, V., 1988, "Application of Hybrid Finite Element Method to Electromagnetic Scattering from Coated Cylinders," IEEE Transactions on Antennas and Propagation, Vol. 36, pp. 50–54.

Kim, C.S., 1991, "Scattering of an Obliquely Incident Wave by a Coated Elliptical Conducting Cylinder," Journal of Electromagnetic Waves and Applications, Vol. 5, pp. 1169–1186.

Lee, Jin-Fa and Cendes, Z.J., 1987, "The Transfinite Element Method for Computing Electromagnetic Scattering From Arbitrary Lossy Cylinders," AP-S International Symposium, paper AP03-5, Blacksburg, Virginia.

Magnus, W., Operhettinger, F. and Soni, R.P., 1966, "Formulas and Theorems for the Special Functions of Mathematical Physics," Springer-Verlag, New York.

Rojas, R., 1988, "Scattering by an Inhomogeneous Dielectric/Ferrite Cylinder of Arbitrary Cross-Section Shape - Oblique Incidence Case," IEEE Transactions on Antennas and Propagation, Vol. 36, pp. 238–246.

Stratton, J.A., 1941, "Electromagnetic Theory," McGraw-Hill, New York.

Temkin, S., 1981, "Elements of Acoustics," John Wiley and Sons, New York.

Toyama, N. and Shogen, K., 1984, "Mathieu Function for Given Parameters and Arguments," IEEE Transactions on Antennas and Propagation, Vol. AP–32, pp. 537–539.

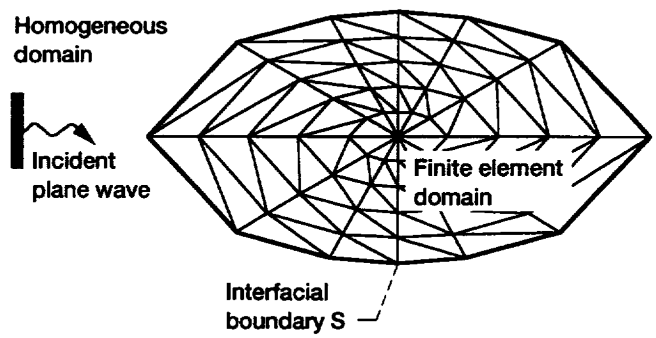

Figure 1.—Finite element grid system.

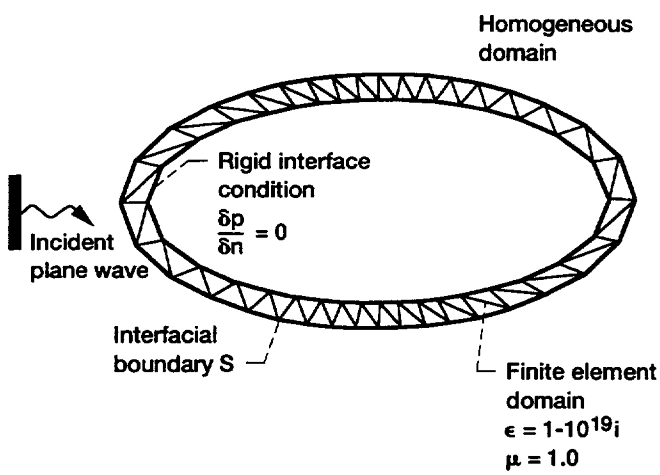

Figure 2.—Finite element ring grid system for rigid bodies.

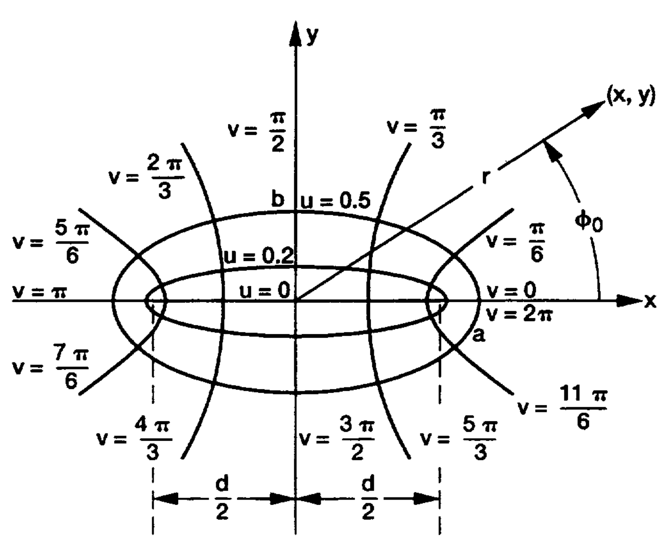

Figure 3.—Elliptic cylindrical geometry.

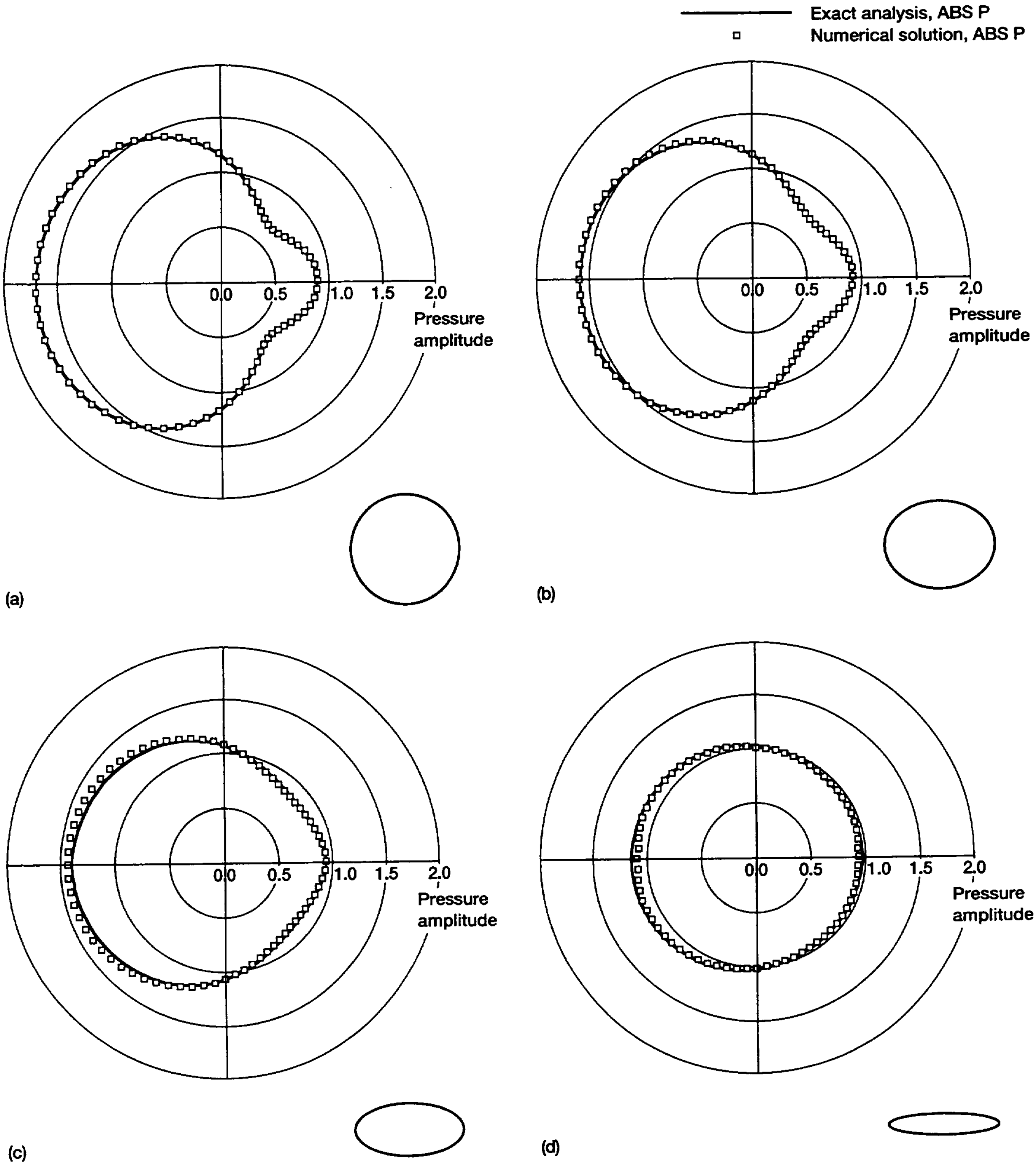

Figure 4.—Near field polar plot of total acoustic pressure around a rigid ellipse subjected to plane wave impingement reconstructed from calculated modal coefficients at specified b (k = 1, a = 1, r = 1.0). (a) b = 1.0. (b) b = 0.8. (c) b = 0.5. (d) b = 0.2.

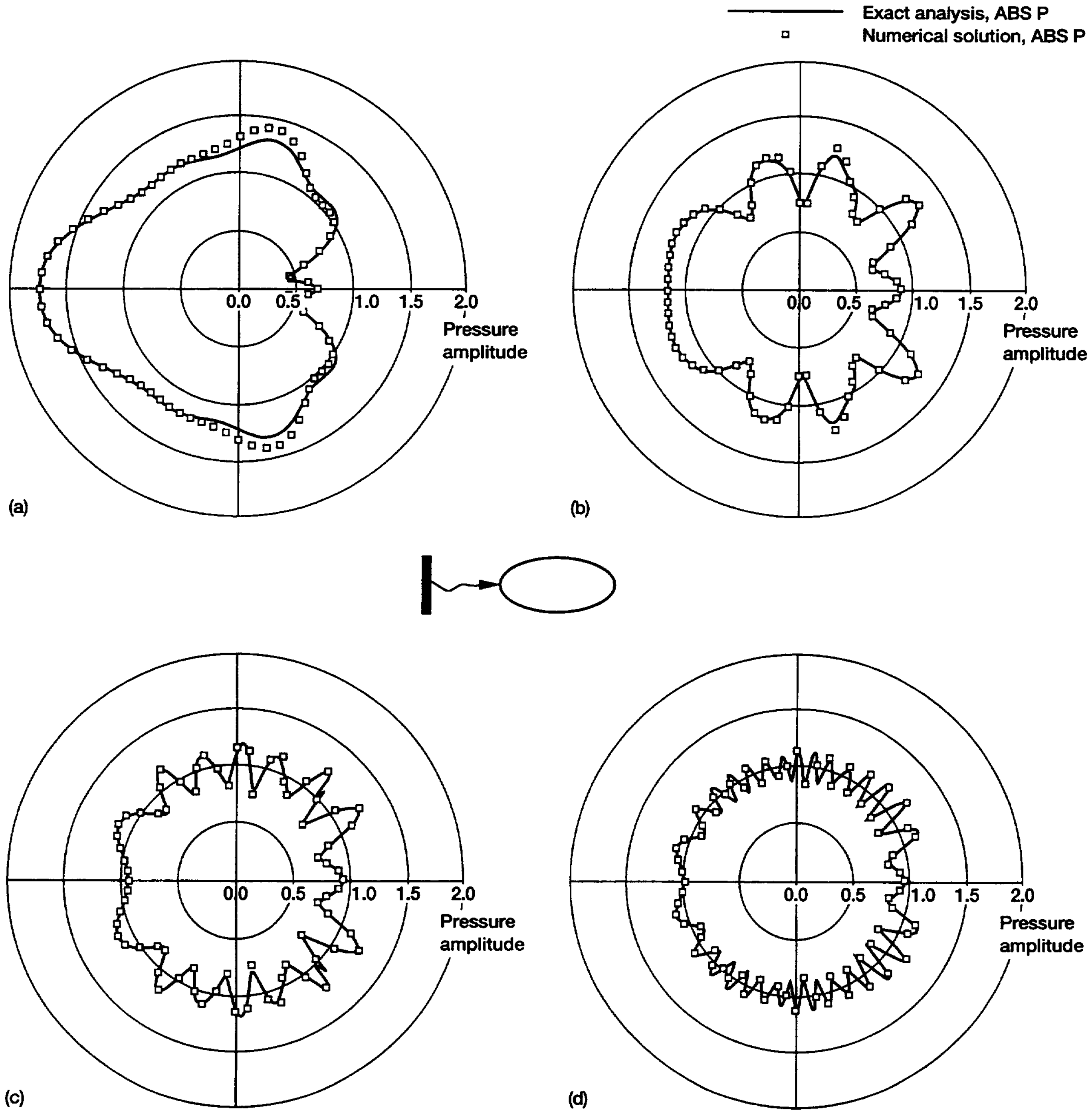

Figure 5.—Polar plot of total acoustic pressure around a rigid ellipse subjected to plane wave impingement reconstructed from calculated modal coefficients at specified radius r (k = 5, a = 1, b = 0.5). (a) r = 1. (b) r = 3. (c) r = 5. (d) r = 10.

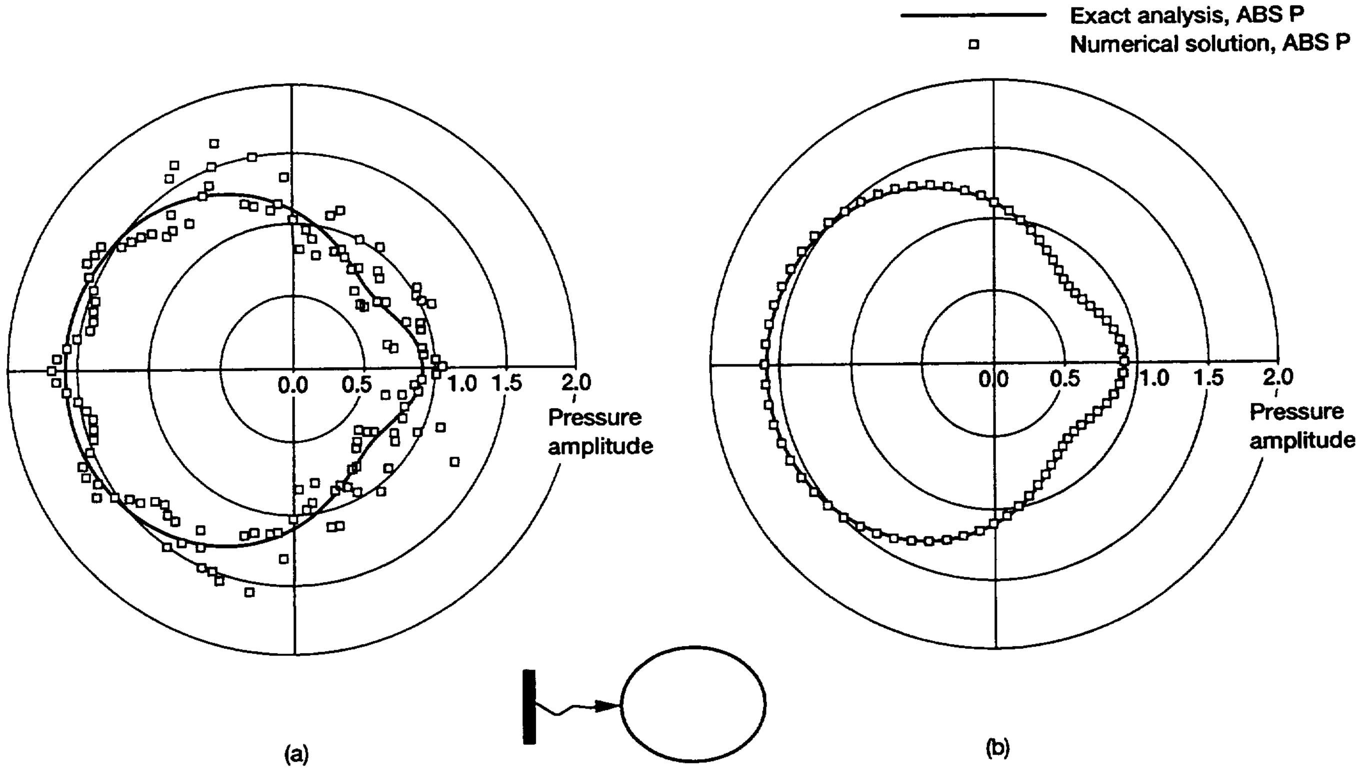

Figure 6.—Total pressure amplitude on the surface of an ellipse subject to plane wave scattering (k = 1, b = 0.8). (a) Finite element solution. (b) Modal solution.

REPORT DOCUMENTATION PAGE

Form Approved
OMB No. 0704-0188

1. AGENCY USE ONLY (*Leave blank*)	2. REPORT DATE	3. REPORT TYPE AND DATES COVERED
	June 1995	Technical Memorandum

4. TITLE AND SUBTITLE

Acoustic Scattering From Ellipses by the Modal Element Method

5. FUNDING NUMBERS

WU–505–62–52

6. AUTHOR(S)

Kevin L. Kreider and Kenneth J. Baumeister

7. PERFORMING ORGANIZATION NAME(S) AND ADDRESS(ES)

National Aeronautics and Space Administration
Lewis Research Center
Cleveland, Ohio 44135–3191

8. PERFORMING ORGANIZATION REPORT NUMBER

E–9663

9. SPONSORING/MONITORING AGENCY NAME(S) AND ADDRESS(ES)

National Aeronautics and Space Administration
Washington, D.C. 20546–0001

10. SPONSORING/MONITORING AGENCY REPORT NUMBER

NASA TM–106935

11. SUPPLEMENTARY NOTES

Kevin L. Kreider, The University of Akron, Department of Mathematical Sciences, Akron, Ohio 44325 and Kenneth J. Baumeister, NASA Lewis Research Center. Responsible person, Kenneth J. Baumeister, organization code 2660, (216) 433–5886.

12a. DISTRIBUTION/AVAILABILITY STATEMENT

Unclassified - Unlimited
Subject Category 71

This publication is available from the NASA Center for Aerospace Information, (301) 621–0390.

12b. DISTRIBUTION CODE

13. ABSTRACT ***(Maximum 200 words)***

The modal element method is used to study acoustic scattering from ellipses, which may be acoustically soft (absorbing) or hard (reflecting). Because exact solutions are available, the results provide a benchmark for algorithm performance for scattering from airfoils and similar shapes. Numerical results for scattering from rigid ellipses are presented for a wide variety of eccentricities at moderate frequencies. These results indicate that the method is practical.

14. SUBJECT TERMS

Finite elements; Modes; Scattering

15. NUMBER OF PAGES

15

16. PRICE CODE

A03

17. SECURITY CLASSIFICATION OF REPORT	18. SECURITY CLASSIFICATION OF THIS PAGE	19. SECURITY CLASSIFICATION OF ABSTRACT	20. LIMITATION OF ABSTRACT
Unclassified	Unclassified	Unclassified	